Available online at www.sciencedirect.com
ScienceDirect
Journal of Sound and Vibration 313 (2008) 631–642
JOURNAL OF SOUND AND VIBRATION
www.elsevier.com/locate/jsvi

A numerical study of 1D self-similar waveguides: Relationship between localization, integrated density of state and the distribution of scatterers

Etienne Bertaud du Chazaud[a,*], Vincent Gibiat[b]

[a] Département Génie Civil, IUT de Cergy Pontoise, F-95031 Cergy Pontoise, Cedex, France
[b] Université Paul Sabatier Toulouse III, PHASE, F-31062 Toulouse, Cedex, France

Received 21 May 2006; received in revised form 25 November 2007; accepted 26 November 2007
Available online 7 January 2008

Abstract

The vibrational behaviour of 1D mechanical structures locally loaded with additional masses according to a self-similar pattern is considered. An analysis of the multiple scattering problem is proposed to point out the existence of strongly localized modes. The eigenfrequency distribution is investigated through the vibrational integrated density of state (integrated DOS). The features of this distribution allow one to predict the mode shapes and give an indication of the additional masses number and weight. Finally, the role played by the distribution of the additional masses in the vibrational behaviour of the structure is discussed.

1. Introduction

Following the pioneering work of Anderson on localization about random systems [1], the vibrational properties of structures presenting a self-similar mass distribution have been widely studied since the beginning of the 1980s [2–5]. In a previous paper [6], has been presented an experimental and numerical study of acoustic propagation in a self-similar waveguide (see Fig. 1a–d) where stop-bands and trapped modes are observed. These modes have been related to a localization phenomenon.

On one hand, such an acoustic waveguide is interesting to analyse and describe the trapping sound waves but it is difficult to perform continuous measurement inside the structure without perturbations to verify the localization hypothesis. On the other hand, the waveguide has the advantage to be easily mimicked by any constant localized mechanical system with the possibility of a simpler experimental realization as well as an analytical description. A mechanical system has been designed on a lattice of identical masses coupled by springs; it converges to a string when the length of the springs leads to zero.[1] Discontinuities are obtained by inserting loading masses at points corresponding to the Cantor set (see Fig. 1e–h). This ‘toy system’ has not

*Corresponding author. Tel.: +33 1 34 25 68 06.
E-mail address: etienne.bertaud@u-cergy.fr (E.B. du Chazaud).
[1] Or the number of masses per unit length leads to infinity.

0022-460X/$ - see front matter
doi:10.1016/j.jsv.2007.11.049

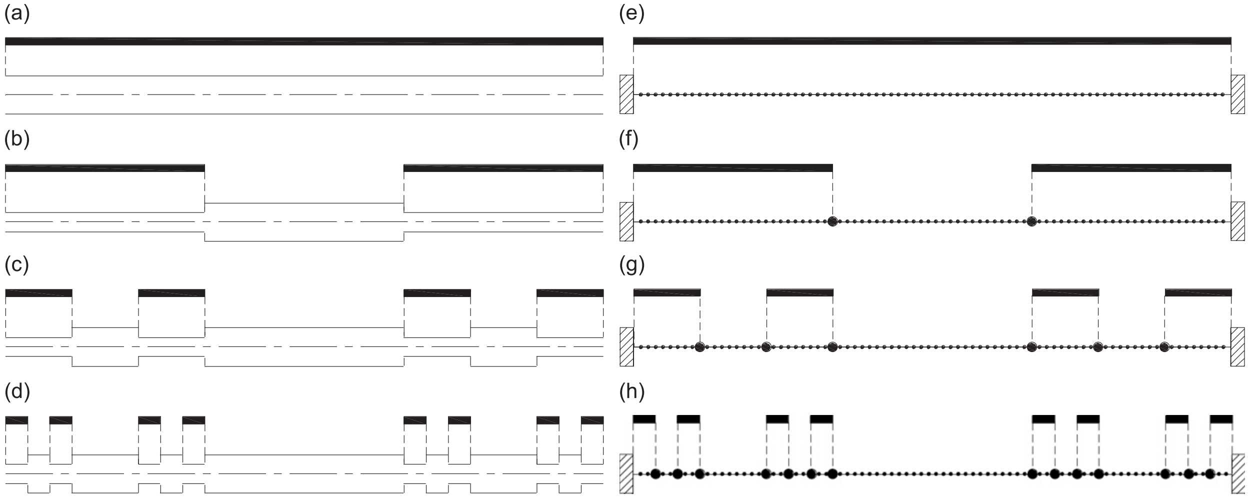

Fig. 1. Order 0, 1, 2 & 3 of the acoustic waveguide (a)–(d) and the mechanical structure (e)–(h). For each structure, the corresponding prefractal figure of the Cantor set is represented with bold segments.

been designed through an iterative process to reproduce a string loaded by masses but to allow simple analytical and numerical study which results on the associated eigenproblem reveals the presence or the absence of localized modes.

Localized and extended modes as well as forbidden bands are an important subject in solid state physics where the properties of crystals [7], quasi-crystals [8–11] and random materials [1] leads to these peculiar properties. Moreover the whole set of these behaviours can be also found on fractal structures. Even if these crystallographic studies are very near of mechanics, only a very few number of references are available in the field of structures and structural mechanics. One can cite without any exhaustivity the works of Bouzit et al. on random structures and that of Fletcher et al. on fractal structures [12–14].

In a first part, the analytical description of the mechanical system is given. Then the solution (in frequency and in space) of the eigenproblem is determined and trapped modes are observed. In a second part, we show that these modes are strongly localized (Section 3). These phenomena will be analysed through the integrated density of state (Section 4). Finally, the properties of a randomized self-similar structure [15] is shown to be almost equivalent to a deterministic self-similar structure of same order n and fractal dimension D (Section 5).

2. The Cantor-like vibrating structure

The Cantor-like vibrating structure is a self-similar object [5,16,17], built through an iterative homothetic process that leads, when iterate to infinity, to a fractal [18,19] as any object built in a same way. When the iterative process is not driven to infinity, the object is a prefractal of order n.

Experimental and numerical evidence of mode trapping has been achieved in a previous acoustical work [6]. A self-similar waveguide is built from an initial pattern made of 3 successive tubes of length $l/3$ and diameter d, D and d ($D>d$) which is amplified and replicated and timed according to the Cantor set to what will be called a Cantor like waveguide of order n (see Figs. 1a–d). The modes of this acoustical waveguide have been explored through impedance and transmission losses measurements, then compared to numerical simulations. The results prove the existence of trapped or maybe localized modes. As it is difficult to visualize the modal acoustic field with sufficient accuracy to verify if the trapped modes are really localized, other experiments or numerical simulations are required. Any change in diameter causes an impedance discontinuity. When sufficiently important, these discontinuities act as scatterers allowing to replace the acoustical problem by 1D multiple scattering one. We develop a mechanical model where tubes of any diameter (called spans) are represented by a constant localized system of identical springs and masses, and where the diameter discontinuities are represented by extra masses. For a unit length mechanical structure, these masses are placed at the edges of the portions of a Cantor set of same prefractal order, as shown in Figs. 1e–h.

The structure is defined by its number of elements N, its length l, its prefractal order n, the mass m of each identical adjacent mass, the mass M of each mass discontinuity and the stiffness κ of each spring. The number p of masses M is

$$p = \sum_{i=1}^{n} 2^i = 2^{n+1} - 2. \tag{1}$$

Two masses M delimit a span; we count $2^{n+1} - 1$ spans in the order n structure. The length $l_{s,i}$ of a span is $l_{s,i} = i \times l/3^n$ with i integer ($i \in [1;n]$).

We define the loading ratio β as

$$\beta = \frac{\text{sum of additional mass}}{\text{mass of the non-loaded chain}} = \frac{p(M-m)}{Nm}. \tag{2}$$

This parameter is another way to characterize masses M and eventually allows to compare structures of different order and same weight. The study is limited to highly loaded structures ($\beta \in [1; +\infty[$).

Considering the harmonic motion of pulsation ω, the transversal displacement $y_i(t) = \hat{y}_i \exp(\mathrm{j}\omega t)$ of the ith mass from its equilibrium position obeys the motion equation:

$$-m_i\omega^2\hat{y}_i + 2\kappa\hat{y}_i - \kappa(\hat{y}_{i-1} + \hat{y}_{i+1}) = 0, \tag{3}$$

with m_i equals to M if i corresponds to a loaded site and to m if it does not. The whole set of equations can be represented through a tri-diagonal dynamical matrix $\mathbf{D}(n, m, \beta, N)$:

$$\mathbf{D}(n, m, \beta, N) \times \left\{ \begin{matrix} \hat{y}_1 \\ \vdots \\ \hat{y}_N \end{matrix} \right\} = \left\{ \begin{matrix} 0 \\ \vdots \\ 0 \end{matrix} \right\}, \tag{4}$$

with $\mathbf{D}(n, m, \beta, N)_{i,i} = 2\kappa/m_i - \omega^2$ and $\mathbf{D}(n, m, \beta, N)_{i\pm1,i} = -\kappa/m_i$.

Considering the matrix:

$$\mathbf{M}(n, m, \beta, N) = \mathbf{D}(n, m, \beta, N) + \omega^2 \cdot \mathbf{I}, \tag{5}$$

with $\mathbf{I}$ the $N \times N$ identical matrix, the roots of the characteristic equation $\det(\mathbf{M}(n, m, \beta, N)) = 0$ are the squared eigenfrequencies ω_k of the problem. The eigenmodes are the eigenvectors of $\mathbf{M}(n, m, \beta, N)$. The numerical solution is straightforward and has no drawback.

The representation of the whole set of the eigenmodes[2] (see Fig. 2 for an order 3 highly loaded structure ($\beta \gg 1$)) shows that for some frequency bandwidths, the wave remains trapped in localized zones of the structure. We define ω_0 as the fundamental frequency of the non-loaded structure. In Fig. 2, for $\omega/\omega_0 < 12$, the behaviour is close to the one of homogeneous structures: the vibration is present in each span and the modes appear extended. Between this frequency and $\omega/\omega_0 \approx 25$, the modes are "trapped": energy is concentrated within the central span or the central span of the lateral parts of the structure. Beyond $\omega/\omega_0 = 25$, the pattern of Fig. 2 is strictly periodic: extended modes alternate with two modes trapped in the central span followed by one mode trapped in the lateral parts.[3] As already observed [3,6], we notice that when energy is trapped in the lateral spans, the central span is motionless, although the lengths of two spans are linked by an integer factor. The structure is intermediate between a periodic system and a random one, as quasi-lattices [8,9,11].

These observations raise two questions: May the mode trapping phenomenon observed be qualified of strong localization? May the particular mode distribution be explained?

[2]This figure is analogous to the representation of the simulated internal pressure distribution for an order 3 Cantor-like waveguide (see Fig. 10 from Ref. [6]).

[3]In fact three trapped modes in the central part and 2 in the lateral one counting the degenerated modes.

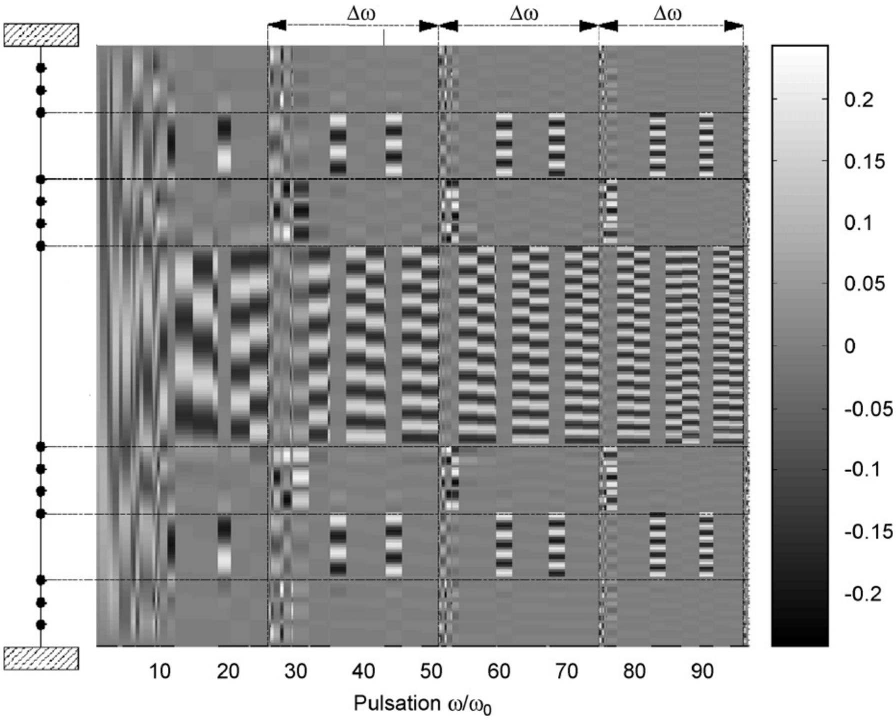

Fig. 2. Set of the $N/2$ first transverse eigenmodes ($\hat{y}_i$) of the order 3 structure ($\beta = 1.15$ and $N = 243$). ω_0 is the fundamental pulsation of the non-loaded structure.

3. Strong localization of the transversal displacement

The trapping phenomenon is clearly observed for modes 21 and 23 of the order 3 structure in Figs. 3a and b. It can be characterized precisely by observing how energy is decaying (in the time domain) at the edges of the concerned spans: Figs. 3c and d clearly show that the decay of the logarithm of the displacement absolute value is linear. Beyond the pth eigenfrequency ω_p ($[0; \omega_p]$ is the first passband of the structure and corresponds to the resonance of the loading masses), the displacement of the masses M is weak and it has been assumed that each of these masses behaves as a scatterer, characterized by a same reflection coefficient R and a same transmission coefficient T [20]; in the case of highly loaded structures, R is much higher than T at any frequency.[4] Out of the trapping zone, a multiple scattering process of the wave leads to its exponential spatial extinction. Considering a wave coming out from a trapped mode span, its amplitude A_i is transmitted[5] with a global transmission coefficient $\mathcal{T}(r)$ (r, distance from a point to the edge of the span):

- at the abscissa $r = 0$, $\mathcal{T}(r) = T(1 + R^2 + R^4 + \mathcal{O}(R^6, T))$,
- at abscissa $r = l/3^n$, $\mathcal{T}(r) = T^2(1 + 2R^2 + 3R^4 + \mathcal{O}(R^6, T))$,
- at abscissa $r = 2l/3^n$, $\mathcal{T}(r) = T^3(1 + 3R^2 + 6R^4 + \mathcal{O}(R^6, T))$,
- and at abscissa $r = 3l/3^n$, $\mathcal{T}(r) = T^4(1 + 3R^2 + 6R^4 + \mathcal{O}(R^6, T))$,

where $\mathcal{O}(R^6, T)$ represents the terms that are neglected. The transmission process does not exactly correspond to a geometric series (that leads an exponential evolution of the transmitted wave); considering that energy is extinguished if the wave amplitude after the fourth scatterer is less than one percent of the initial wave, we

[4] In fact, it is easy to show [20] that for any value of $\beta > 0$, R tends to 1 as frequency increase; localization exists for lightly loaded structure if it is possible to study eigenmodes at high frequency.

[5] Considering the transmission process after 6 of 7 steps where one step correspond to $l/(c \times 3^n)$ and c is the wave celerity.

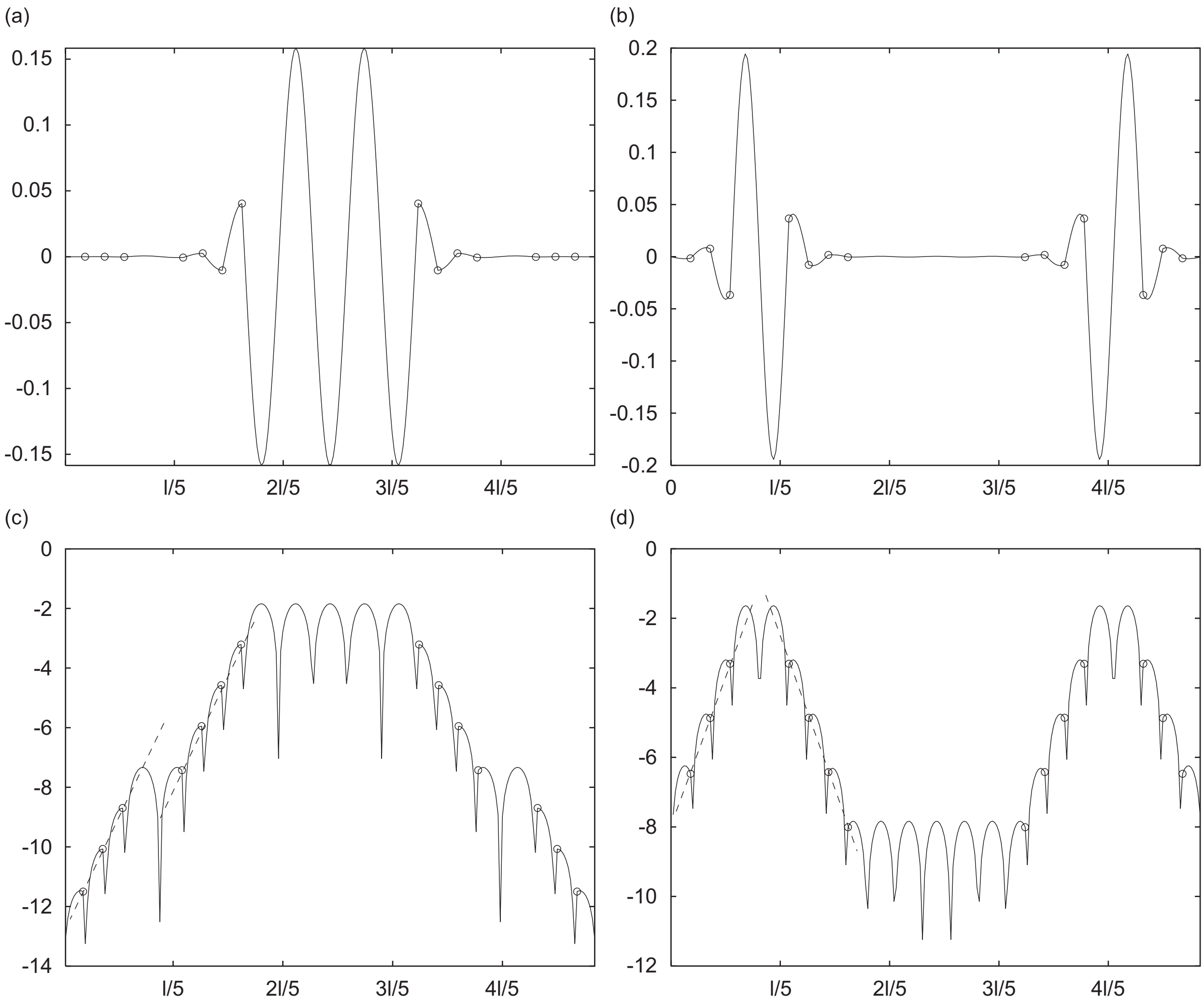

Fig. 3. Shape and Log-shape of the displacement (the circles correspond to scatterers positions): (a) mode $21 - \omega/\omega_0 = 15.0$, (b) mode $23 - \omega/\omega_0 = 18.4$, (c) mode $21 - \log(|y_i(\omega)|)$, (d) mode $23 - \log(|y_i(\omega)|)$.

Table 1
Numerical study of the global transmission process ($T = 0.204$)

r	0	$l/3^n$	$2l/3^n$	$3l/3^n$
$\mathscr{T}(r)$	0.536	0.263	0.120	0.038
$\log(\mathscr{T}(r))$	−0.271	−0.580	−0.920	−1.415

assume $T^4(1+3R^2+6R^4) \leqslant 0.01$ that gives $T \leqslant 0.204$ and $R = 1 - T \geqslant 0.796$. Table 1 represents the numerical values of $\mathscr{T}(r)$ and $\log(\mathscr{T}(r))$ in this case. The correlation coefficient between r and $Y = \log(\mathscr{T}(r))$ is $\rho_{r,Y} = \mathrm{cov}(r, Y)/(\sigma_r \sigma_Y)$ with $\mathrm{cov}(x, y)$ covariance of populations x and y and σ_x standard deviation of population x; with Table 1 values, we obtain $\rho_{r,Y} \approx -0.993$. The linear relation linking r and Y leads to an exponential relation between r and $\mathscr{T}(r)$; the decay of energy outside the considered span is exponential. This can be written as

$$y_i(r) \approx A_i \exp(-r \times \mathrm{f}(R)) \quad \text{and} \quad \mathscr{T} \ll 1, \tag{6}$$

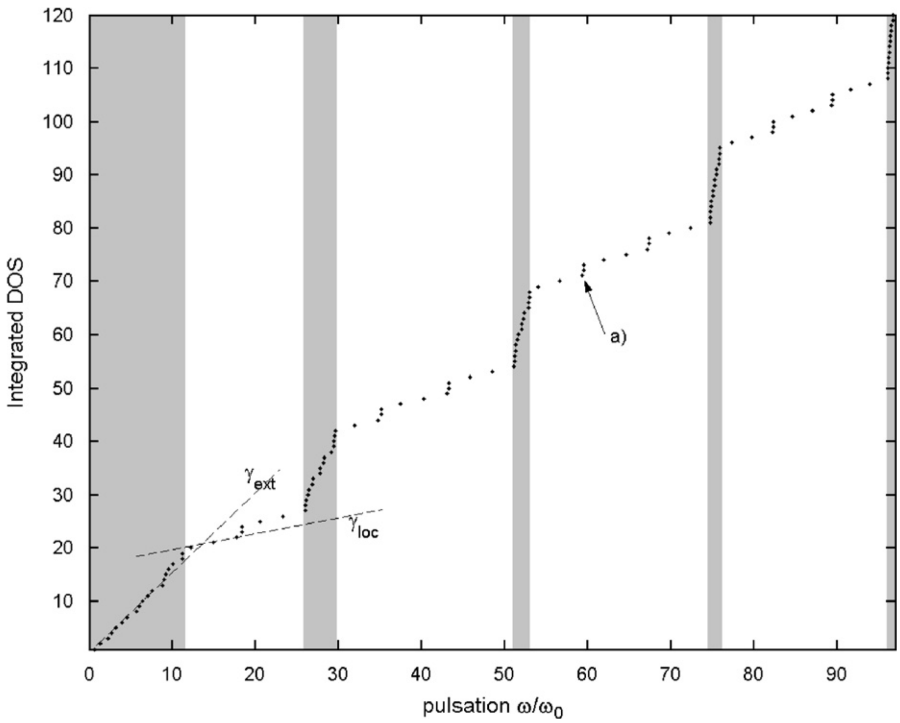

Fig. 4. Integrated DOS of the order 3 structure (the $N/2$ first modes; $\beta = 1.15$ and $N = 243$): (a) correspond to localization in lateral spans.

with $f(x)$, function of x. $d_L = 1/f(R)$ is defined as the length of localization. The expression of $y_i(r)$ is then:

$$y_i(r) \approx A_i \exp\left(-\frac{r}{d_L}\right). \tag{7}$$

This expression is similar to the decay formulation of Anderson [1].

In such self-similar structures, mode trapping corresponds to an exponential extinction of the displacement and consequently to a strong localization phenomenon. In that case, the rapid decay of energy at the edges of the localization zone prevents wave from propagating outside the span and it is not transmitted; the structure behaves as a stop-band filter.

4. Integrated density of state: cross-overs and devil staircase-like shape

4.1. Cross-overs

The integrated density of state[6] (integrated DOS) $I(\omega)$ represents, for a given system at a given frequency ω, the number of eigenmodes that can be found in the frequency interval $[0;\omega]$. This parameter is often used to identify the nature (extended, localized) of the modes since frequency distribution and mode shape are highly linked [2,8]. For homogeneous structures, according to Debye law [21], we get $\log(I(\omega)) \propto d \log(\omega)$, with d the euclidean space dimension in which the structure is embedded. It has been shown that for mass fractal structures and on the range of length where the fractal pattern is observed [2,22], localized modes distribution leads to $\log(I(\omega)) \propto \bar{d} \log(\omega)$ with $\bar{d}$ defined as the spectral dimension [2,23]. This dimension $\bar{d} = 2D/(2+\delta)$ is obtained with D the fractal dimension of the structure and δ a parameter characteristic of its geometry and its connectivity; one finds $\bar{d} < d$ for $d > 1$ and $\bar{d} = d$ for $d = 1$.

[6]Also known as integrated density of mode.

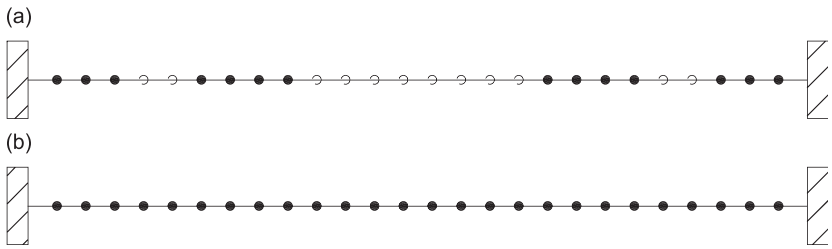

Fig. 5. Comparison between two close structures: (a) order 3 self-similar structure; (b) periodic structure.

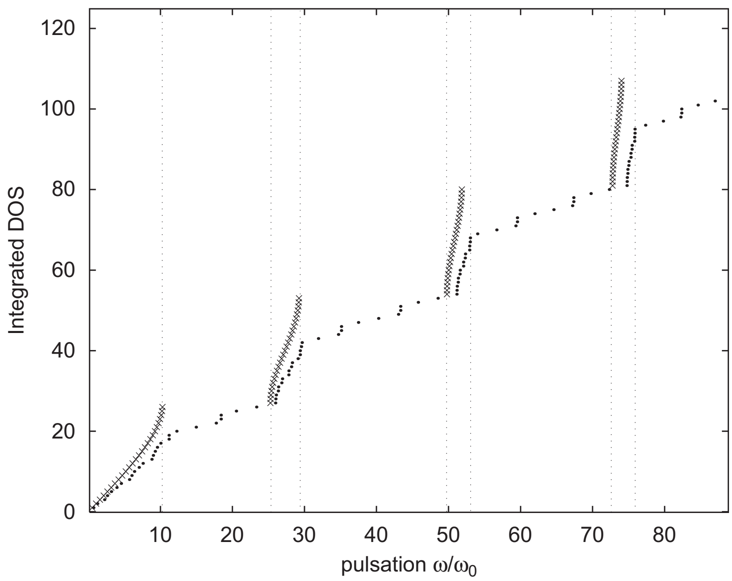

Fig. 6. Representation of the Integrated DOS of a periodic and a self-similar structure ($N/2$ first modes; $\beta = 1.15$ and $N = 243$): $\times$ deterministic, $\bullet$ self-similar. The dotted lines delimit the extended mode zones of the two structures.

Fig. 4 represents the integrated DOS $I(\omega)$ of the order 3 structure, presented at Section 2. The shaded zones correspond to extended mode bandwidths. Numerous slope crossovers give the figure a stair-like shape; the extended mode slopes (Fig. 4, slopes γ_{ext}) are much higher than the localized mode ones (Fig. 4, slopes γ_{loc}). Using a precise analysis of the mode shapes, we show that these crossovers do not correspond here to any spectral dimension value.

The vibrating behaviour of periodic structures such as the one shown in Fig. 5b is well known [21]: all the modes of their spectrum are extended and appear in pass bands separated by large band gaps. The first pass band corresponds to a mode family called ‘‘acoustic phonon mode’’ while the others describe a second one called ‘‘optical phonon mode’’ [21].

Comparing the integrated DOS of a prefractal order 3 structure to a fully periodic structure of same length (these two structures are shown in Fig. 5 while their integrated DOS appear in Fig. 6), it appears that the branches of the extended modes are nearly the same.[7] The integrated DOS of the extended zones of the prefractal structures is well described by the integrated DOS of the periodic structure; this one is deduced from the dispersion relation of the structure ($I \propto k$, with k the wavenumber) since, for 1D structures, the wave number is linked to the order of the mode in the spectrum. Among these extended modes, we find localized ones. Fig. 6 shows that the localized modes of the prefractal structure[8] appear in the band gaps of the periodic

[7]Their heights are different because there are more extended modes in a periodic structure (there are more extra masses).
[8]Because of its periodicity, the periodic structure do not possess any localized mode.

structure showing how the structures studied are intermediate between periodic and random structures. If the exponential decay is fast enough, we can make the approximation that, at low frequency, the localized modes are nothing but simple string modes within the structure.

Each set of modes previously described obeys to a specific dispersion relation. For the extended modes, the dispersion relations of acoustic and optical phonon modes are well known [21]. They are not linear but their maximum slope $\Delta\omega/\Delta k$ is the one of the acoustical modes at low frequency, which corresponds to the dispersion law of a continue string of same weight [8]. This slope is proportional to the inverse of the minimum slope $\Delta I/\Delta\omega$ of the integrated DOS I. For the localized modes, since they also correspond to simple string modes, their dispersion relation as well as their integrated DOS are known. We get:

$$\frac{\Delta I}{\Delta\omega_{\text{ext,opt}}} > \frac{\Delta I}{\Delta\omega_{\text{ext,acou}}} \propto l_p\sqrt{\rho_p} \text{ as well as} \frac{\Delta I}{\Delta\omega_{\text{loc}}} \propto l_p\sqrt{\rho_p}, \tag{8}$$

where l_p is the length of the vibrating part and ρ_p its density. $(\Delta I/\Delta\omega_{\text{loc}})$ is always smaller than $(\Delta I/\Delta\omega_{\text{ext}})$ because for the localized modes the length l_p appears shorter (the wave settles in a limited zone of the structure) and the density ρ_p slighter (the localization excludes the loading masses from the shape). Transition from an extended modes zone to a localized one actually corresponds to a crossover in the integrated DOS. These crossovers do not correspond to a particular value of the spectral dimension $\bar{d}$ as this parameter is equal to the euclidean dimension d for a mono-dimensional structure ($\bar{d} = d = 1$, see Refs. [2,23]).

4.2. Identification of the vibrating spans in localized modes

Other information on the vibrating behaviour is available from the integrated DOS. For $\beta \to \infty$ (condition that actually turns to M mass to absolute reflective scatterer), any vibration that settles within the span of length l_s also settles in spans of length $3^k \times l_s$, with k integer. For β finite but high ($\beta > 1$), these degenerations turn to quasi-degenerations. Localized modes in shorter spans than the central one are always frequentially close to a set of modes localized in longer spans; we observe quasi-vertical zones in the integrated DOS curve (see Fig. 4, mark a). In these zones, ΔI, the number of quasi-degenerated modes for a given ω, can consequently be deduced from the numbering of the different spans of the structure considered. The $2^{n+1} - 1$ spans in the structure are linked to each other by scale factors multiple of 3:

$$\begin{cases} 3 \times 2^{n-1} & \text{spans of length } l/3^n \text{ (the shorter spans)}, \\ 2^{n-j} & \text{spans of length } l/3^{n+1-j}\ (j \in [2;n]). \end{cases} \tag{9}$$

Since localization concerns spans longer than $l/3^n$ (vibration in the shorter spans leads to extended modes), we obtain:

$$\Delta I = \sum_{j=i}^{n} 2^{n-j} = 2^{n-i}, \tag{10}$$

with i identifying the span of length $l_s = l/3^{n+1-i}$, shorter span concerned by the vibration at ω (i in $[1;n]$). Consequently, we can find the different spans concerned by the localization from the heigh of a quasi vertical zone in the integrated DOS. As the modes are quasi-degenerated, the experimental identification of these zones can be difficult (in case of important noise and low-quality factor resonances); anyway, they have already been observed [3].

4.3. Devil staircase-like shape

For orders higher than 3, an analysis around the self-similarity can also be processed. The integrated DOS of an order 5 structure is represented in Fig. 7. We can observe that it is possible to magnify successively (twice from Fig. 7b) the figure with a constant scale ratio $\xi \approx 3$ and to observe the same pattern (a devil staircase-like curve with three large steps). The self-similar character of the structure signs its physical behaviour. It is interesting to notice that this curve is close to the integrated DOS of a Fibonacci scheme structure which also corresponds to a Cantor-like spectrum [8]. Moreover, the Hausdorff dimension D of the model used to place

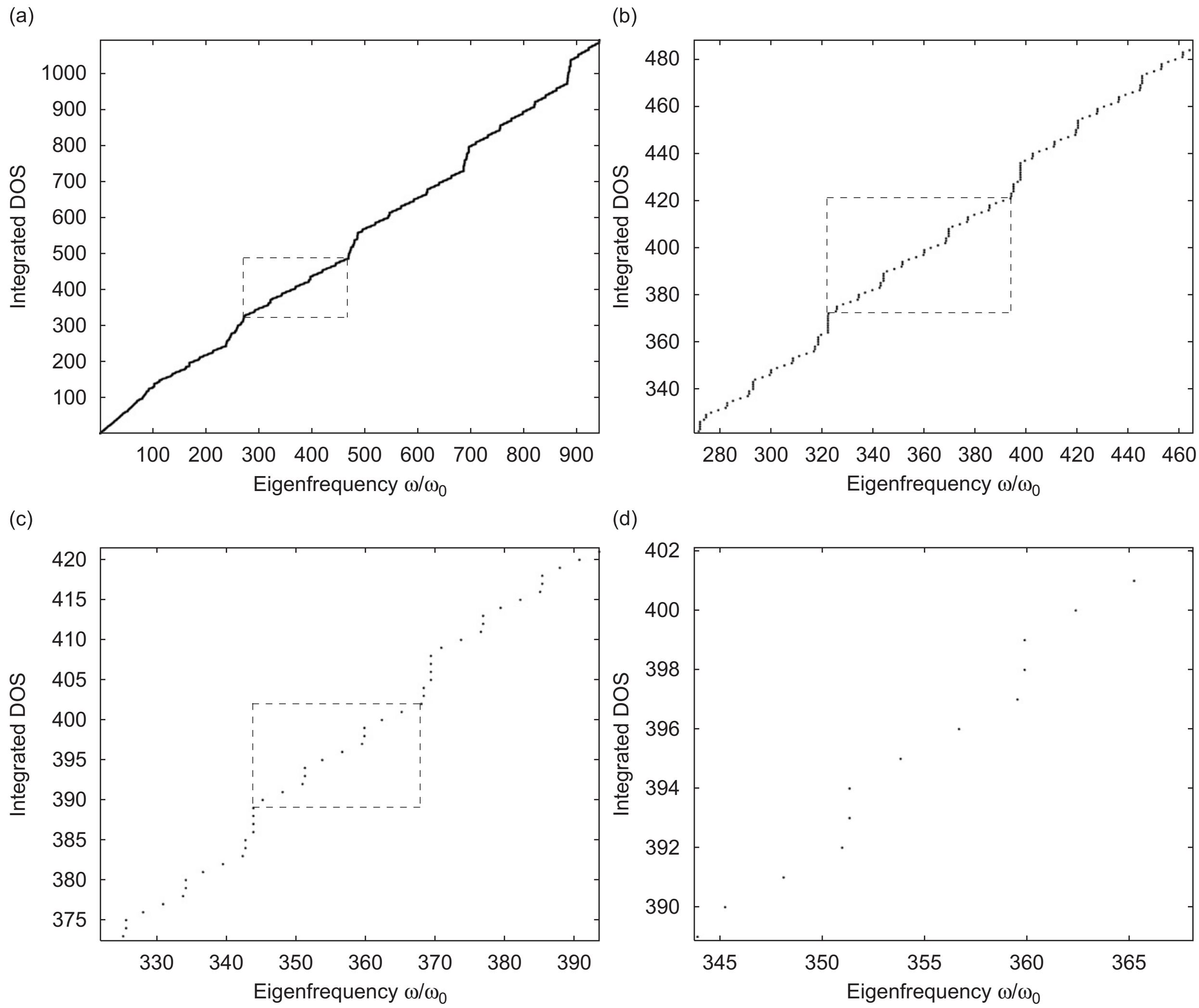

Fig. 7. Integrated DOS of the order 5 structure ($\beta = 1.15$ and $N = 2187$): (a) plot on $[0; N/2]$; (b) zoom on the frame of panel a, (c) zoom on the frame of panel b, (d) zoom on the frame of panel c.

the masses M (the Cantor Set) and its prefractal order n can be deduced from the scale ratio ξ, from the observation of the invariant pattern and from the number of successive magnification that it is possible to process. Finally, the value of the spectral dimension ($\bar{d} = 1$) is confirmed because in a linear axis system, the parts of the curve corresponding to localization are linear.

5. Role of the distribution of the scatterers

A question remains concerning the role of the scatterers distribution in the behaviour of the structure. The deterministic[9] structures presented in the previous sections present strong localization. Among other phenomena, it is important to explore the consequences of the geometrical regularity of the structure.

A random fractal structure can be derived from the previous deterministic self-similar structure by a random permutation of the different spans, so that their number, their length and the number of loading

[9]A deterministic process leads to their construction.

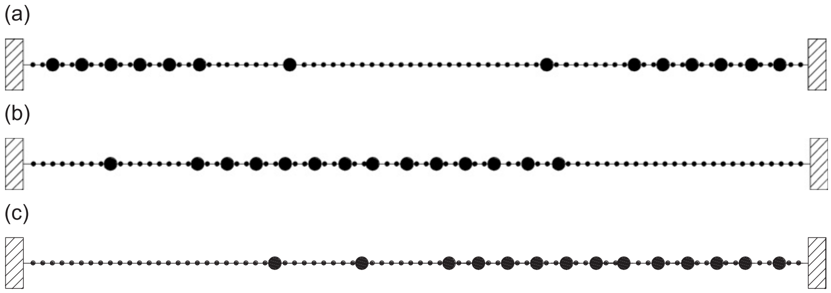

Fig. 8. Three different distributions of the scatterers of an order 3 self-similar structure.

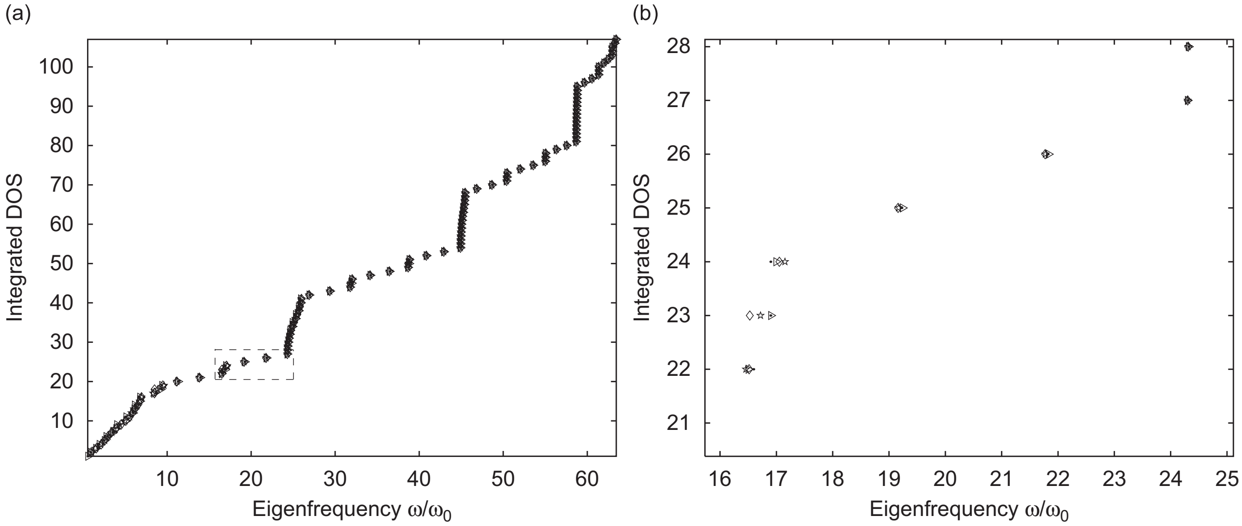

Fig. 9. Integrated density of state of the structures presented in Fig. 8 ($\beta = 1.15$): (a) global view; (b) zoom on the dashed frame of (a). • Deterministic, ▷ distribution of (a), ◇ distribution of (b), ⋆ distribution of (c).

masses M are unchanged. For a given order n, numerous distributions are possible. Fig. 8 presents 3 different distributions for an order 3 self-similar structure:

- Masses gathered at the centre of the structure (Fig. 8a).
- Masses gathered at the edges of the structure (Fig. 8b and c).
- Central and lateral spans adjacent (Fig. 8b and c).
- Central and lateral spans separated (Fig. 8a).

These distributions appear extreme as most of the scatterers are gathered but the behaviour of any other structures shall anyway be intermediate between the behaviour of these ones and the behaviour of the deterministic one. The different curves presented in Fig. 9 and comparing an order 3 deterministic structure and the random ones presented in Fig. 8 are similar. The eigenfrequencies of the different structures so appear to be independent from the distribution.

The case of infinitely heavy scatterers represents the limit behaviour of any structure since the value of the reflection coefficient R of mass M tends to 1 as ω increase (and it increase faster and faster as β increase). For infinitely heavy scatterers, the characteristic polynomial of the vibrational problem is

$$\det(\mathbf{M}(n,m,\beta\to\infty,N)) = (\omega^2)^p \prod_i \det(\mathbf{M}(0,m,1,N_i)).$$

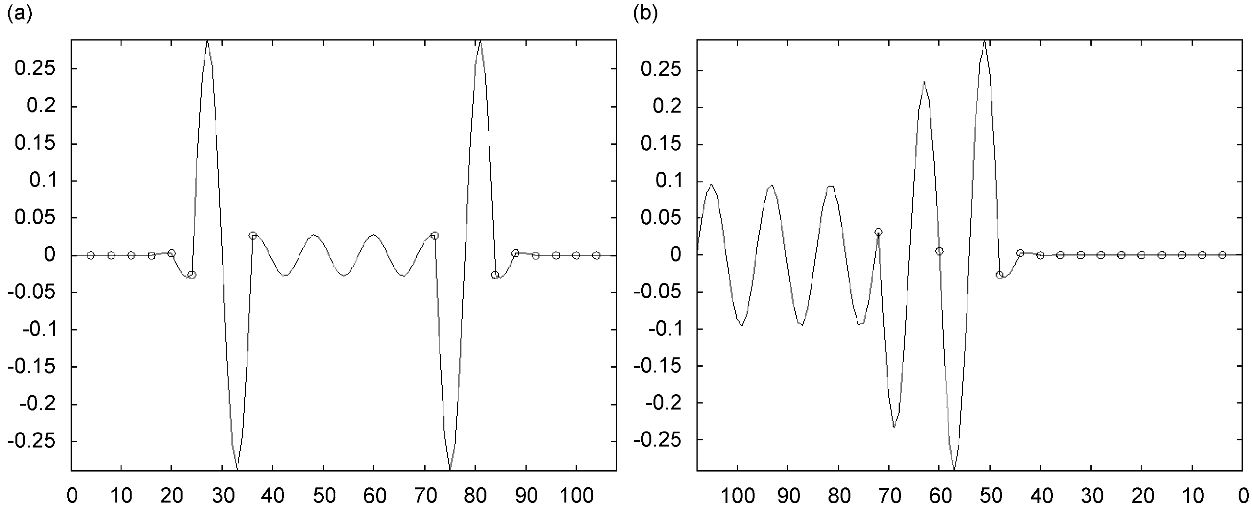

Fig. 10. Mode 23 ($\omega/\omega_0 = 18.4$) of two order 3 prefractal structures (to be compared with Fig. 3b); $\beta = 1.15$: (a) corresponds to the distribution presented in Fig. 8a, (b) corresponds to the distribution presented in Fig. 8c.

Since the multiplication is commutative, the eigenvalues of matrix $\mathbf{M}(0, 1, N_i)$ that describe non-loaded structures of N_i elements (the different spans of the structure) are independent from the distribution (all the scatterers are motionless).

For finite-weight structures (and $\beta > 1$), we observe extended (acoustical and optical) and localized modes. Acoustical modes are known to be nearly independent from loading masses positions and the four distributions possess the same eigenfrequencies in this pass-band. Furthermore, the permutations processed keep spans length unchanged: optical modes are also unchanged in these distributions (since loading masses sites correspond to nodes in these modes).

Finally in the localized modes, few scatterers contribute to the wave extinction. The localization is close to a redefinition of the limits of the structure that can be cut at a very short distance from the edges of the vibrating span. The position of the span in the structure is therefore without effects for this type of modes.

The case of secondary localizations (localizations in the lateral spans) has to be discussed. For the deterministic structures, we observe that excitation of the lateral spans is exclusive of excitation of the central part, despite the integer multiple factor of scale that exists between these two families. For the structures of Figs. 8b and c, only one scatterer separates the two families of spans. In this case, the displacement in the lateral spans cannot be extinguished before entering the central one which is then excited as shown in Fig. 10. Anyway, the mode is still localized, even if the part concerned by the excitation is greater.

6. Conclusions

Extended and trapped modes are observed in the spectrum of 1D self-similar structures. They appear intermediate between periodic and random systems, like quasi-periodic structures previously studied [8,9]. Considering the scattering process, we show that wave trapping corresponds to a strong localization phenomenon that prevents vibrational energy transmission and introduces stop-band in such structures. The analysis of the integrated density of state allows one to predict the localization bandwidths since the wave trapping corresponds to abrupt crossovers, where origin does not correspond to any weak value of a spectral dimension $\bar{d}$. As for the quasi-periodic structures based on a Fibonacci scheme, we find that the curve fits a devil staircase-like figure; this result is more evident for the self-similar system as it is based on the same model as the devil staircase (the Cantor set). Fractal dimension D and prefractal order n can be extracted. We finally show that the deterministic character of the structure does not interfere with its vibrating behaviour: any distribution of scatterers leading to a fractal dimension D and a prefractal order n behaves the same way.

Possible application of localized modes have not yet be explored but the capacity of these structures to trap energy at some frequencies let us imagine multiple noise filtering applications.

References

[1] P.W. Anderson, Absence of diffusion in certain random lattices, *Physical Reviews* 109 (1958) 1492–1505.
[2] S. Alexander, R. Orbach, Density of states on fractals: fractons, *Journal de Physique Lettre* 43 (1982) L625–L631.
[3] A. Alippi, A. Petri, A. Bettucci, F. Craciun, F. Farrelly, E. Molinari, Vibrational properties of a continuous self-similar structure, *Physical Review B* 49–21 (1994) 15067–15075.
[4] A. Alippi, A. Petri, A. Bettucci, F. Craciun, F. Farrelly, E. Molinari, Direct experimental observation of fracton mode patterns in one-dimensional cantor composites, *Physical Review Letters* 68–10 (1992) 1555–1558.
[5] B. Sapoval, S. Santra, J.J.S. Andrade, Additivity of vibrational density of states in two-dimensional mesoscopic systems, *Physical Review B* 63 (2001) 060301(R).
[6] V. Gibiat, A. Barjau, K. Castor, E.B.D. Chazaud, Acoustical propagation in a prefractal waveguide, *Physical Review E* 67 (2003) 066609.
[7] L. Brillouin, *Wave Propagation in Periodic Structures*, McGraw-Hill, New York, 1946.
[8] J.P. Lu, T. Odagaki, J.L. Birman, Properties of one-dimensional quasilattices, *Physical Review B* 33 (7) (1986) 4809.
[9] J.P. Lu, J.L. Birman, Acoustic-wave propagation in quasiperiodic, incommensurate and random systems, *Physical Review B* 38 (12) (1988) 8067.
[10] G. Gumbs, M.K. Ali, Dynamical maps, cantor spectra and localization for fibonacci and related quasiperiodic lattices, *Physical Review Letters* 60 (11) (1988) 1081–1084.
[11] E. Maciá, Thermal conductivity of one-dimensional fibonacci quasicrystals, *Physical Review B* 61 (10) (2000) 6645–6653.
[12] D. Bouzit, C. Pierre, Localization of vibration in disordered multi-span beams with damping, *Journal of Sound and Vibration* 187 (1994) 625–648.
[13] D. Bouzit, C. Pierre, Wave localization and conversion phenomena in multi-coupled multi-span beams, *Chaos, Solitons and Fractals* 11 (2000) 1575–1596.
[14] N.H. Fletcher, T. Tarnopolskaya, F.R. de Hoog, Wave propagation on helices and hyperhelices: a fractal regression, *Proceedings of the Royal Society of London A.*
[15] M. Filoche, B. Sapoval, Transfer across random versus deterministic fractal interfaces, *Physical Review Letter* 84–25 (2000) 5776–5779.
[16] B. Sapoval, T. Gobron, A. Margolina, Vibrations of fractal drums, *Physical Review Letters* 67–21 (1991) 2974–2977.
[17] B. Sapoval, T. Gobron, Vibrations of strongly irregular or fractal resonators, *Physical Review E* 47–5 (1993) 3013–3024.
[18] B. Mandelbrot, *Les Objets Fractals*, Flammarion, 1982.
[19] B. Mandelbrot, *The fractal geometry of nature*, Freeman, New York, 1982.
[20] P.M. Morse, K.U. Ingard, *Theorical Acoustics*, Princeton University Press, Princeton, NJ, 1968.
[21] C. Kittel, *Introduction to Solid State Physics*, Wiley, New York, 1996.
[22] R. Vacher, E. Courtens, G. Coddens, A. Heidemann, Y. Tsujimi, J. Pelous, M. Foret, Crossovers in the density of states of fractal silica aerogels, *Physical Review Letters* 65–8 (1990) 1008–1011.
[23] R. Rammal, G. Toulouse, Random walks on fractal structures and percolation clusters, *Journal de Physique Lettre* 44 (1983) L13–L22.